Polymer Bulletin (2021) 78:5741–5753
https://doi.org/10.1007/s00289-020-03395-x

ORIGINAL PAPER

Preparation of SBA-15 surface lanthanum ion-imprinted polymer and its adsorption properties

Longlong Yue[1] · Qian Xie[1] · Yifeng Yang[1] · Jing Li[1] · Xiancai Li[1]

Received: 31 October 2019 / Revised: 31 August 2020 / Accepted: 30 September 2020 /
Published online: 9 October 2020

Abstract

The preparation of a lanthanum ion-imprinted polymer is described via surface ion imprinting, with polyethyleneimine as the functional monomer and SBA-15 as the matrix material. Its structure was characterized and analyzed, and static adsorption experiments were carried out to determine the best experimental conditions for the adsorption of lanthanum ions. The effects of initial concentration, temperature, adsorption time and pH on the adsorption of lanthanum ion surface-imprinted polymer were investigated. In addition, the regeneration performance of La(III)-IIP-PEI/SBA-15 on lanthanum ion was studied and showed that La(III)-IIP-PEI/SBA-15 has strong specific recognition ability and high reuse performance.

Keywords Surface ion imprinting · Polyethyleneimine · SBA-15 · Specific recognition ability

Introduction

SBA-15 is an important constituent of SBA series-type mesoporous molecular sieves [1]. Its structure is identical to that of MCM-41 mesoporous molecular sieves, both of which are two-dimensional hexagonal structures [2–6]. Due to improved hydrothermal stability, SBA-15 is widely used in catalytic and adsorption reactions. Sewage is commonly treated with adsorption technology [7], and its efficiency can be improved by using SBA-15. Due to the simple operation and high adsorption capacity of the adsorbent, the adsorption method has become the most effective in treating rare earth ion contamination [8].

SBA-15 molecular sieve was first synthesized by Academician Zhao [9] in 1998. The step of synthesizing SBA-15 molecular sieve requires two parts: The first part is to form a liquid crystal phase in solution through active agent molecules (such as P123) containing hydrophilic and hydrophobic groups at both ends and inorganic

✉ Xiancai Li
xcli@ncu.edu.cn

[1] College of Chemistry, Nanchang University, Nanchang 330031, People's Republic of China

monomer molecules under a certain condition. Organic–inorganic liquid crystal phase: At this time, the structure of the sample has a lattice parameter of nanometer size. The second part uses high-temperature heat treatment to remove the organic template, and the sample will form a highly ordered pore structure.

So far, there are three main methods for preparing SBA-15 molecular sieves: hydrothermal synthesis [10, 11], sol–gel method and microwave radiation method. The hydrothermal synthesis method is a reaction of an acid solution, a templating agent and a silicon source in a constant temperature water bath. After a certain period of time, it is crystallized, washed, filtered and dried. Next, the template is calcined by high temperature to obtain a mesoporous material.

The research focus of surface ion-imprinted materials is primarily on how to increase the adsorption capacity of materials [12], enhance the selection performance and regeneration performance of adsorbent adsorption [13], optimize the optimal adsorption experimental conditions [14], simplify the recovery [15], more efficiently separate and purify within the process [16] and other aspects [17, 18]. The high selectivity of surface ion-imprinted polymers has made surface imprinting technology increasingly useful in the field of wastewater treatment.

Polyethyleneimine (PEI) contains amine groups in its molecular backbone, which can form strong coordination with rare earth metal ions [19–21]. PEI is a solid material that can capture heavy metal ions and rare earth ions. Examples of studies of the adsorption of heavy metal ions by polyethyleneimine are PEI coated on ion exchange resin and silica gel surfaces [22–24].

At present, the main method used for rare earth separation is solvent extraction, but according to our understanding, solvent extraction is not only inefficient, but also not environmentally friendly. Therefore, it is very important to choose an efficient and environmentally friendly separation method. In this paper, a surface ion-imprinting technique was used to synthesize a lanthanum ion surface ion-imprinted polymer with good selective adsorption properties for lanthanum ions, which achieved separation and enrichment of rare earth lanthanum ions.

Experimental

Chemicals and reagents

Tetraethyl orthosilicate (TEOS, 98%), surfactant poly(ethylene glycol)-block-poly(propylene glycol)-block-poly(ethylene glycol)(P123), $La(NO_3)_3{\cdot}6H_2O$, $Gd(NO_3)_3{\cdot}6H_2O$, $Ce(NO_3)_3{\cdot}6H_2O$ and $Pr(NO_3)_3{\cdot}6H_2O$ were all obtained from Sinopharm Chemical Reagent Co., Ltd. 3-chloropropyltriethoxysilane and epichlorohydrin were obtained from Aladdin Reagent. Hydrochloric acid (HCl), $Al(NO_3)_3{\cdot}9H_2O$ and $Fe(NO_3)_3{\cdot}9H_2O$ were purchased from Xilong Scientific Co., Ltd. Distilled water was used throughout.

Preparation La(III)-IIP-PEI/SBA-15

Preparation of alkylated SBA-15

Alkylated SBA-15 matrix material was prepared under acidic conditions using P123 as the template, ethyl orthosilicate as the silicon source and 3-chloropropyltriethoxysilane as the coupling agent. 2.01 g of P123 was weighed with an analytical balance and added to a 500-mL three-neck flask. Then, 50 mL of deionized water and 10.4 mL of concentrated hydrochloric acid were added to the three-necked flask and stirred until the P123 was dissolved in a constant temperature water bath at 40 °C. After 1 h, 4.25 mL of tetraethyl orthosilicate was added dropwise to the three-necked flask, and the mixture was vigorously stirred for 1 h. Next, 0.45 mL of 3-chloropropyltriethoxysilane was pipetted slowly into the mixed system and stirred for 22 h. The solution was poured hot into a clean 500-mL large beaker and statically crystallized for two days at room temperature. It was suction filtered, washed repeatedly with deionized water and dried overnight at 75 °C to obtain a white powder. According to the standard of adding 1.5 g of raw powder per 200 mL of ethanol solution, Soxhlet was extracted with ethanol at 80 °C for 6 h and dried to obtain alkylated SBA-15.

Preparation of PEI/SBA-15

2.5 g of polyethyleneimine was dissolved in 100 mL of deionized water, and the alkylated SBA-15 obtained in "Preparation of alkylated SBA-15" section was mixed therein and stirred in a water bath at 90 °C for 10 h. After the reaction completed, it was cooled and repeatedly rinsed with deionized water to remove the remaining PEI. PEI/SBA-15 was obtained and dried at 80 °C overnight.

La(III)-imprinted PEI/SBA-15

The dried PEI/SBA-15 was added to a higher concentration of La^{3+} (100 mL, 1000 mg/L) solution and the pH was adjusted to 5. After the adsorption was saturated, the remaining La^{3+} on the surface was washed with deionized water, and then thoroughly dried in a vacuum drying oven at 60 °C and removed.

Preparation of non-ion-imprinted polymers(NIP-PEI/SBA-15)

The step of adsorbing La(III) ions was omitted, while the remaining steps were identical as described in "Preparation La(III)-IIP-PEI/SBA-15" section.

Adsorption procedure

Static adsorption experiment

Thirty milliliters of the low concentration La^{3+} solution was added to a 250-mL Erlenmeyer flask 10 mg of the ground adsorbent was then added, and the conical

flask with plastic wrap. The mixture was shaken for 2 h in a constant temperature water bath shaker until the adsorption reached equilibrium, then centrifuged in a low speed centrifuge, where a certain amount of the supernatant was diluted into a 25-mL volumetric flask and measured by arsenazo(III) colorimetry. The absorbance of the diluted solution was calculated and the concentration of cesium ions in the remaining solution was calculated to determine the adsorption capacity. The formula for adsorption amount is as follows:

$$Q = \frac{(C_0 - C_e)V}{m}, \tag{1}$$

where Q is the adsorption amount of the adsorbent (mg g^{-1}), C_0 is the initial concentration of the rare earth ion (mg L^{-1}), C_e is the concentration of the lanthanum ion at saturation (mg L^{-1}), V is the volume of the sample (L), and m is the mass (g) of the added adsorbent.

Selective identification of lanthanum ions

La^{3+} was separately placed in Gd^{3+}, Ce^{3+}, Pr^{3+}, Y^{3+}, Fe^{3+} and Al^{3+} as a binary coexisting system, and ion-imprinted polymer or non-ion-imprinted polymer was added for sufficient adsorption, where the concentration of each ion was determined by inductively coupled plasma atomic emission spectroscopy (ICP-AES). The partition coefficient, K_d, of each metal ion was determined using Formula (2), the selectivity coefficient k of the ion-imprinted polymer to La^{3+} was calculated according to Formula (3), and then, the specific recognition ability of ion-imprinted polymer to La^{3+} was evaluated.

$$K_d = \frac{Q_e}{C_e} \tag{2}$$

$$k = \frac{K_d(\mathrm{La})}{K_d(\mathrm{M})}, \tag{3}$$

where K_d is the partition coefficient of a specific metal ion, Q_e is the saturated adsorption capacity of the metal ion (mg g^{-1}), C_e is the concentration of the ion at equilibrium (mg L^{-1}), and k is the selectivity of the La^{3+} coefficient.

Characterization methods

The adsorbent was characterized by Fourier transform infrared spectroscopy and scanning electron microscopy; the concentration of rare earth ions in the solution was measured using a spectrophotometer, and the concentration of some mixed ions was measured by inductively coupled plasma atomic emission spectroscopy (ICP-AES).

Results and discussion

Characterizations of adsorbents

Infrared spectroscopy analysis

Figure 1 shows the infrared spectra of SBA-15, PEI/SBA-15 and La^{3+}-IIP-PEI/SBA-15. It is shown that the absorption peaks appearing at 462 cm^{-1}, 806 cm^{-1} and 1090 cm^{-1} are all vibration peaks of Si–O–Si. The peaks at 3420 cm^{-1} and 1630 cm^{-1} can be assigned to the stretching vibration and bending vibration of the alcoholic hydroxyl group on the surface of SBA-15, respectively. The peak appearing at 1420 cm^{-1} is the stretching vibration absorption peak of the C–N bond, and the peak appearing at 1630 cm^{-1} is the bending vibration peak of the N–H bond. All of these indicate that polyethyleneimine has been grafted onto the surface of the SBA-15 molecular sieve to form grafted PEI/SBA-15 particles. The newly emerging peak at 2926 cm^{-1} may be the C–H stretching vibrational peak of the methine formed in the epichlorohydrin reaction.

SEM analysis

Figure 2 shows the SEM images of the adsorbents. La^{3+}-IIP-PEI/SBA-15 showed a rough, uneven surface with noticeable cavities and pore. The difference in NIP-PEI/SBA-15 indicates that the eluent successfully separated the template La(III) ions from the polymer, resulting in many pores [25–27].

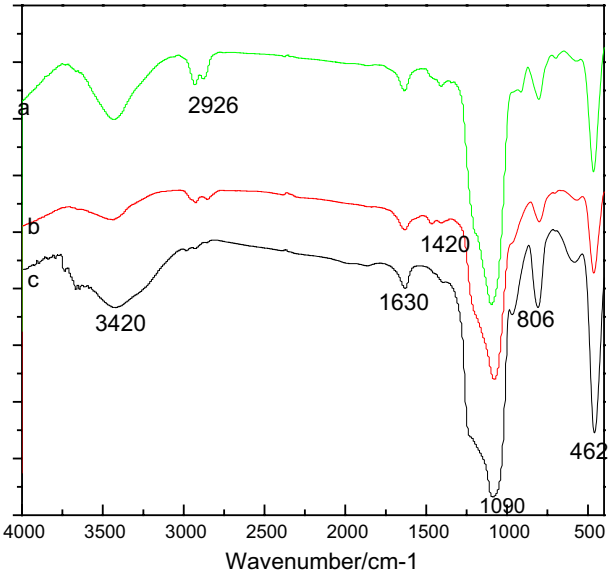

Fig. 1 The infrared spectra of SBA-15 (**a**), PEI/SBA-15 (**b**) and La^{3+}-IIP-PEI/SBA-15 (**c**)

Effect of adsorption conditions on static adsorption properties of adsorbents

Effect of solution pH on adsorption process

For the adsorption process of rare earth ions, the pH of the system must be considered, because pH not only affects the form of rare earth ions in aqueous solution, but also affects the adsorption performance of the adsorbent itself. Rare earth ions are generally present in the form of ions in an acidic solution and ions slowly begin to precipitate in alkaline solution. In this experiment, five samples of the same concentration of La(III) ion solution were prepared, and the pH of the solution was adjusted from 2 to 6 using a pH acidity meter. Then, static adsorption experiments were carried out.

The adsorption amount of La^{3+}-IIP-PEI/SBA-15 was greatest when pH = 5 (Fig. 3). When pH is low, the concentration of H^+ in the solution is high, which forms a coordination with –NH– in the polyethyleneimine, thus causing no blotting of La^{3+}. As pH increased, the H^+ content in the solution decreased, and most of the –NH– was released, thereby increasing the adsorption amount. When the pH continued to rise, the content of OH^- increased, which formed precipitates with La^{3+} leading to decreased adsorption.

Adsorption kinetics study

The relationship between the adsorption of La^{3+}-IIP-PEI/SBA-15 and reaction time is observed in Fig. 4. It can be concluded that the optimum adsorption time is 1 h. To investigate the adsorption mechanism of rare earth ions and the rate limiting step of the adsorption process, the kinetics of adsorption changes with time [28, 29], and the relevant parameters are shown in Table 1.

The fitting parameters of the dynamic model of Table 1 indicate that the correlation coefficient of the quasi-secondary dynamics is closer to 1. Therefore, it can

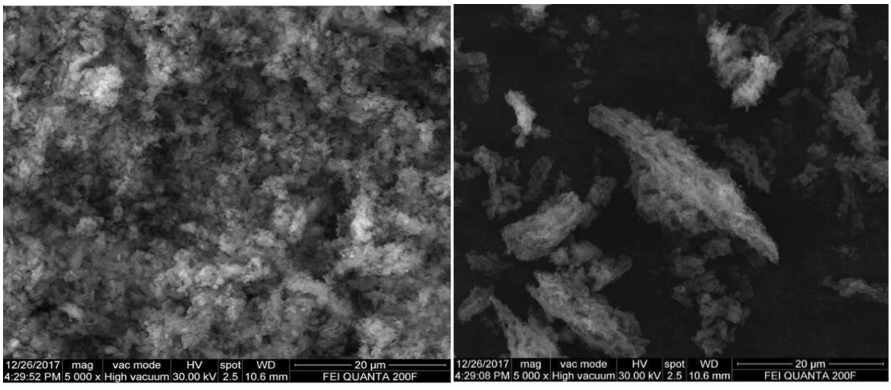

Fig. 2 The SEM images

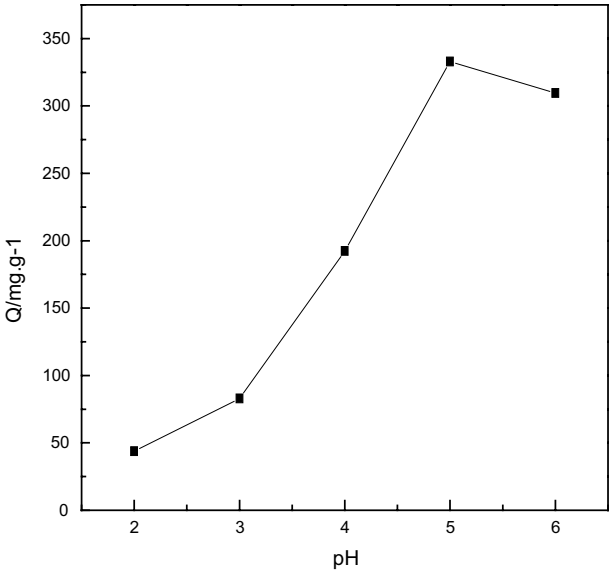

Fig. 3 Effect of pH on the adsorption properties of imprinted material

be assumed that the adsorption of La(III) ions by La^{3+}-IIP-PEI/SBA-15 was more suitable for the quasi-secondary kinetic model. It also indicates that the rate limiting step of the adsorption process of La^{3+}-IIP-PEI/SBA-15 was chemisorption.

Isothermal adsorption model of La^{3+}-IIP-PEI/SBA-15

The adsorption of La^{3+}-IIP-PEI/SBA-15 was carried out at 25 °C, 45 °C and 65 °C (Fig. 5). The adsorption amount rapidly increased with the increase in initial concentration and then more slowly increased ending in a plateau. Adsorption saturation was achieved at an initial concentration of 500 mg L^{-1}, and the adsorption amount reached 629.85 mg g^{-1} at 65 °C.

From the correlation coefficients of the two models in Table 2, the adsorption of La^{3+} by La^{3+}-IIP-PEI/SBA-15 was more consistent with the Langmuir model, and the adsorption of La^{3+}-IIP-PEI/SBA-15 was monolayer adsorption.

Adsorption thermodynamics study of La^{3+}-IIP-PEI/SBA-15

The adsorption thermodynamic constants of La^{3+}-IIP-PEI/SBA-15 at all temperatures are shown in Table 3. ΔG^0 was less than zero, indicating that the adsorption reaction of La^{3+}-IIP-PEI/SBA-15 on La(III) ions can be spontaneously carried out at 25 °C, 45 °C and 65 °C.

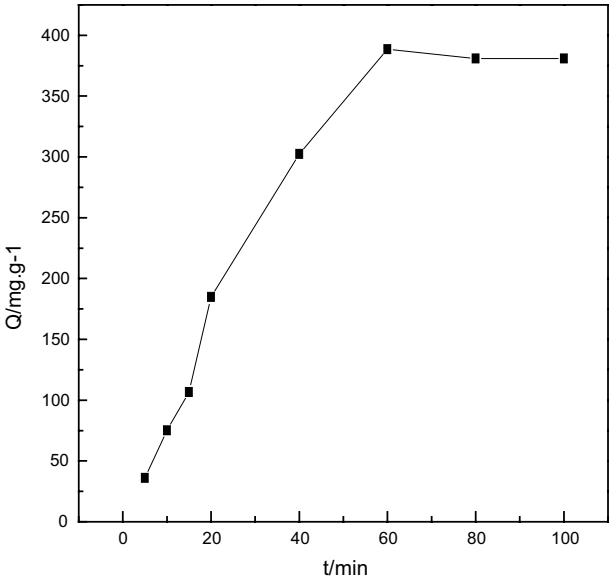

Fig. 4 Time curve of imprinted material

Table 1 Quasi-first-order, quasi-secondary dynamics fitting parameters of imprinted material

Pseudo-first-order equation			Pseudo-second-order equation		
k_1 min^{-1}	R^2	Q_m (mg g^{-1})	$k_2 \times 10^{-4}$/g (mg $min)^{-1}$	R^2	Q_m(mg g^{-1})
0.0268	0.9536	483.96	6.28	0.9978	526.32

Dubinin–Radushkevich (D–R) adsorption model

The adsorption energies, E, of La^{3+}-IIP-PEI/SBA-15 were higher than 8.0 kJ mol^{-1} at 25 °C, 45 °C and 65 °C in Table 4. Thus, the adsorption of La^{3+}-IIP-PEI/SBA-15 was chemical adsorption, which was consistent with the results obtained by the adsorption kinetics.

Selectivity study

The selectivity coefficient of SBA-15 reveals that SBA-15 has almost no selectivity for rare earth ions in Table 5.

As seen in Tables 6 and 7, La^{3+}-IIP-PEI/SBA-15 showed good selectivity to rare earth La(III) ions compared to La^{3+}-NIP-PEI/SBA-15. La^{3+}-IIP-PEI/SBA-15 showed good separation of La^{3+} adjacent to Ce^{3+} and Pr^{3+}, while La^{3+}-NIP-PEI/SBA-15 was not ideal for mixed ion separation. Thus, it was demonstrated that the

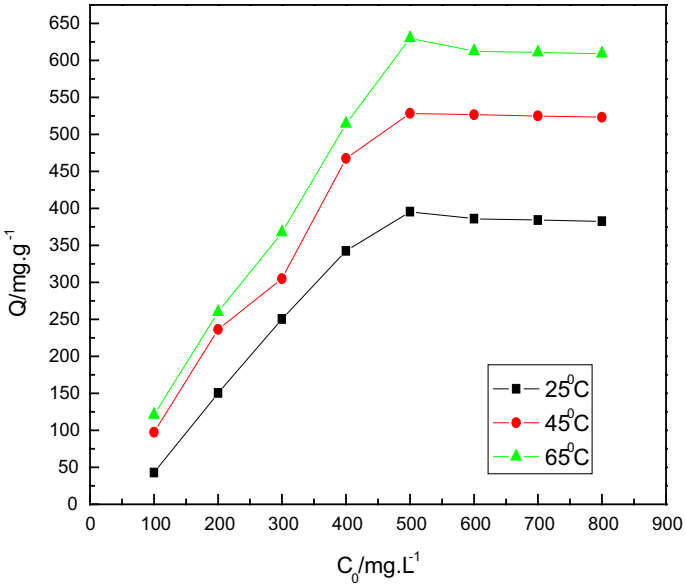

Fig. 5 Isothermal adsorption curve of imprinted material

Table 2 Isotherm fitting parameters of La^{3+}-IIP-PEI/SBA-15 at different temperatures

Adsorption model	Temperature (°C)		
	25	45	65
Langmuir			
R^2	0.9846	0.9904	0.9996
Q_m	416.67	555.56	588.24
K_L	0.0208	0.02145	0.0394
R^2	0.9827	0.9794	0.9972
Freundlich			
n	1.63	1.08	1.03
K_F	8.9245	1.167	1.341

Table 3 Thermodynamic fitting parameters

T (°C)	ΔG^0 (kJ mol^{-1})	ΔS^0 [J (mol K)$^{-1}$]	ΔH (kJ mol^{-1})
25	− 19.63		
45	− 21.83	109.87	13.107
65	− 24.03		

Table 4 Adsorption energies

T (°C)	E (kJ mol^{-1})
25	9.23
45	10.68
65	8.82

Table 5 Distribution coefficient and selectivity coefficient of SBA-15

La^{3+}/M^{3+}	$K_d(La^{3+})$ (mL g^{-1})	$K_d(M^{3+})$	k
La^{3+}/Fe^{3+}	1285.7	358.13	3.59
La^{3+}/Al^{3+}	1166.67	300.69	3.88
La^{3+}/Ce^{3+}	1164.2	1552.27	0.75
La^{3+}/Pr^{3+}	1226.5	1238.89	0.99
La^{3+}/Gd^{3+}	1311.76	1298.77	1.01
La^{3+}/Y^{3+}	1254.9	1140.82	1.10

Table 6 Partition coefficient and selectivity coefficient of La^{3+}-IIP-PEI/SBA-15

La^{3+}/M^{3+}	$K_d(La^{3+})$ (mL g^{-1})	$K_d(M^{3+})$	k
La^{3+}/Fe^{3+}	1025	67.97	15.08
La^{3+}/Al^{3+}	1124.16	42.28	26.59
La^{3+}/Ce^{3+}	1054.8	446.95	2.36
La^{3+}/Pr^{3+}	1216.5	550.45	2.21
La^{3+}/Gd^{3+}	1152.58	377.90	3.05
La^{3+}/Y^{3+}	1214.08	298.30	4.07

Table 7 Partition coefficient and selectivity coefficient of La^{3+}-NIP-PEI/SBA-15

La^{3+}/M^{3+}	$K_d(La^{3+})$ (mL g^{-1})	$K_d(M^{3+})$	k
La^{3+}/Fe^{3+}	1002.65	421.28	2.38
La^{3+}/Al^{3+}	1140.21	440.24	2.59
La^{3+}/Ce^{3+}	1145.28	1156.85	0.99
La^{3+}/Pr^{3+}	1128.6	1064.72	1.06
La^{3+}/Gd^{3+}	1232.05	1062.11	1.16
La^{3+}/Y^{3+}	1015.29	646.68	1.57

ion-imprinted polymer successfully established the blotting site on the surface of the SBA-15 during the preparation process.

Elution and reuse

Sulfuric acid, hydrochloric acid, nitric acid and EDTA were selected as the desorption liquid. Figure 6 demonstrates that the desorption capacity of hydrochloric acid

was the strongest. Five repeated performance tests were carried out using hydrochloric acid as the desorption liquid, and the adsorption rate was still higher than 80%. It is proved that La^{3+}-IIP-PEI/SBA-15 had good regenerative ability and can be reused many times.

Conclusions

The surface ion-imprinting technique was used to prepare the La(III)-imprinted polymer with polyethyleneimine as the functional monomer and SBA-15 as the matrix material. The structure was analyzed and the static adsorption experiment was carried out to determine the best experimental conditions. The conclusions are as follows:

1. The optima pH value for adsorption of low concentration rare earth ion solution was 5, and the optimal adsorption temperature was 65 °C,
2. Via linear fitting of experimental data, the quasi-secondary kinetic model can best describe the adsorption mode of La^{3+}-IIP-PEI/SBA-15,
3. The adsorption of La^{3+}-IIP-PEI/SBA-15 correlated well with the Langmuir isotherm adsorption model, and the thermodynamic analysis of the adsorption process showed that $\Delta G^0 < 0$, which proved that the reaction was spontaneous,
4. Selective adsorption experiments were carried out on matrix materials SBA-15, La^{3+}-IIP-PEI/SBA-15 and La^{3+}-NIP-PEI/SBA-15. It was concluded that La^{3+}-IIP-PEI/SBA-15 had good specific recognition ability for La^{3+}.
5. The desorption properties of different eluents for La^{3+}-IIP-PEI/SBA-15 were investigated, with the finding that the desorption capacity of hydrochloric acid

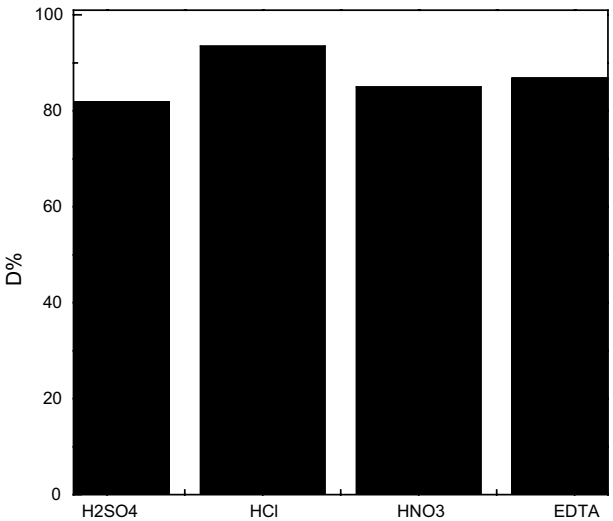

Fig. 6 Elution of imprinted material

is the strongest. Five times of repeated use experiments were carried out with hydrochloric acid, and the adsorption rate was more than 80%, indicating that La^{3+}-IIP-PEI/SBA-15 had good recyclability.

Acknowledgements This work was supported by the Nature Science Foundation of China (51664042).

References

1. Chen LY, Jaenicke S, Gk C (1997) Thermal and hydrothermal stability of framework-substituted MCM-41 mesoporous materials. Microporous Mater 12(4–6):323–330
2. Diaz L, Marquez-Alvarez C, Mohino F, Perez-Pariente J, Sastre E (2001) A novel synthesis route of well ordered, sulfur-bearing MCM-41 catalysts involving mixtures of neutral and cationic surfactants. Microporous Mesoporous Mater 44–45:295–302
3. Zhao D, Feng J, Huo Q, Melosh N, Fredrickson GH, Chmelka BF, Stucky GD (1998) Triblock Copolymer syntheses of mesoporous silica with periodic 50 to 300 angstrom pores. Science 279(5350):548–552
4. Zhao DY, Huo QS, Feng JL, Chmelka BF, Stucky GD (1998) Nonionic triblock and star diblock copolymer and oligomeric surfactant syntheses of highly ordered, hydrothermally stable, mesoporous silica structures. J Am Chem Soc 120(24):6024–6036
5. Sow B, Hamoudi S, Kaliaguine S (2005) 1-Butanol etherification over sulfonated mesostructured silica and organo-silica. Microporous Mesoporous Mater 79(1–3):129–136
6. Wu SJ, Li FT, Zhang B (2010) Research progress in the application of mesoporous adsorbent to the field of water treatment. Ind Water Treat 30(04):1–48
7. Lam KF, Yeung KL, Mckay G (2006) A Rational approach in the design of selective mesoporous adsorbents. Langmuir 22(23):9632–9641
8. Aguado J, Arsuaga JM, Arencibia A (2008) Influence of synthesis conditions on mercury adsorption capacity of propylthiol functionalized SBA-15 obtained by co-condensation. Microporous Mesoporous Mater 109:513–524
9. Zhao D, Huo Q, Feng J (1998) Nonionic triblock and star diblock copolymer and oligomeric surfactant syntheses of highly ordered, hydrothermally stable, mesoporous silica structures. J Am Chem Soc 120(24):6024–6036
10. Hang M, Wang S-Q, Wu S-J et al (2005) Advences of nanoscale rare earth materials. Inner Mong Petrochem Ind 06:3–4
11. Chen Z-H (2000) Rare earth new materials and their application in the field of high technology. Chin Rare Earths 01(55–59):1
12. Awual MR, Rahman IM, Yaita T et al (2014) pH dependent Cu(II) and Pd(II) ions detection and removal from aqueous media by an efficient mesoporous adsorbent. Chem Eng J 236:100–109
13. Wang J, Liu F (2014) Enhanced and selective adsorption of heavy metal ions on ion-imprinted simultaneous interpenetrating network hydrogels. Des Monomers Polym 17(1):19–25
14. Pirouz MJ, Beyki MH, Shemirani F (2015) Anhydride functionalised calcium ferrite nanoparticles: a new selective magnetic material for enrichment of lead ions from water and food samples. Food Chem 170:131–137
15. Wu XW, Ma HW, Yang J (2012) Adsorption of Pb(II) from aqueous solution by a poly-elemental mesoporous adsorbent. Appl Surf Sci 258:5516–5521
16. Buhani N, Nuryono KE et al (2010) Production of metal ion imprinted polymer from mercapto-silica through sol-gel process as selective adsorbent of cadmium. Desalination 251:83–89
17. Guo M, Wang C-G, Yao S-S et al (2015) Synthesis of ion imprinted polymers with carbon nanotubes and their ion recognition performance. J Chem Eng Chin Univ 04:155–161
18. Bisset W, Jacobs H, Koshti N, Stark P, Gopalan A (2003) Synthesis and metal ion complexation properties of a novel polyethyleneimine *N*-methylhydroxamic acid water soluble polymer. React Funct Polym 55:109–119
19. Radi S, Ramdani A, Lekchiri Y, Morcellet M, Crini G, Janus L, Martel B (2000) Preparation of pyrazole compounds for attachment to chelating resins. J Appl Polym Sci 78:2495–2499

20. Chanda M, Rempel GL (1995) Polyethyleneimine gel-coat on silica. High uranium capacity and fast kinetics of gel-coated resin. React Polym 25:25–36
21. Amara M, Kerdjoudj H (2004) Separation and recovery of heavy metals using a cation-exchange resin in the presence of organic macro-cations. Desalination 168:195–200
22. Amara M, Kerdjoudj H (2002) Modified cation exchange resin applied to demineralisation of a liquid industrial waste. Comparison to a classical treatment and electrodialysis. Hydrometallurgy 65:59–68
23. An F, Gao B (2008) Adsorption of phenol on a novel adsorption material PEI/SiO_2. J Hazard Mater 152(3):1186–1191
24. Zheng X-M, Fan R-Y, Xu Z-K (2012) Preparation and property evaluation of Pb(II) ion-imprinted composite membranes. Acta Polym Sin 05:561–570
25. Lambert A, Macquarrie DJ, Carr G et al (2000) The catalytic oxidation of cyclohexanone to caprolactone using hexagonal mesoporous silica supported SbF_3. New J Chem 24(7):485–488
26. Kantipuly C, Katragadda S, Chow A et al (1990) Chelating polymers and related supports for separation and preconcentration of trace metals. Talanta 37(5):491–517
27. Wang Y, Yu A, Tan Z et al (2005) Synthesis and application of cross-linked polyvinyl alcohol derivative for adsorption of Europium(III). Ion Exch Adsorpt 21(1):33–39
28. Zhou YI (2005) Rare-earth Elements and APPlication in the Hi-Tech Field. Yinshan Acad J 19(03):27–28, 34
29. Zhang M, Wang S-Q, Wu S-J et al (2005) Advences of nanoscale rare earth materials. Inner Mongolia Petrochem Ind 06:3–4